Simulation Modelling Practice and Theory 18 (2010) 836–849

Contents lists available at ScienceDirect

Simulation Modelling Practice and Theory

journal homepage: www.elsevier.com/locate/simpat

Surge arresters' circuit models review and their application to a Hellenic 150 kV transmission line

C.A. Christodoulou [a], L. Ekonomou [b,*], A.D. Mitropoulou [a], V. Vita [b], I.A. Stathopulos [a]

[a] National Technical University of Athens, School of Electrical and Computer Engineering, High Voltage Laboratory, 9 Iroon Politechniou St., Zografou Campus, 157 80 Athens, Greece
[b] A.S.PE.T.E. – School of Pedagogical and Technological Education, Department of Electrical Engineering Educators, N. Heraklion, 141 21 Athens, Greece

ARTICLE INFO

Article history:
Received 31 July 2009
Received in revised form 27 January 2010
Accepted 28 January 2010
Available online 4 February 2010

Keywords:
Surge arresters
Simulation
Transmission lines
Failure probability
Models

ABSTRACT

Metal oxide surge arresters are used to protect medium and high voltage systems and equipment against lightning and switching overvoltages. Measurements of the residual voltage of the metal oxide surge arresters indicate dynamic characteristics with the residual voltage to increase as the current front time descends and the residual voltage to reach its maximum, before the arrester current reaches its peak. Thus, the metal oxide surge arresters cannot be modeled by only a non-linear resistance, since its response depends on the magnitude and the rate of rise of the surge pulse. Several frequent dependent models have been proposed, in order to simulate this dynamic frequency-dependent behavior. This study constitutes a review of the most important models, which are tested using PSCAD. The residual voltage of each model, implying 5 kA, 10 kA and 20 kA 8/20 μs impulse current, is compared with the manufacturers' datasheet. The models are also used to study the lightning performance of a Hellenic 150 kV transmission line with the arresters implemented on every one, two or three towers, calculating their failure probability. The results show that all models function with a satisfactory accuracy and the differences among the models arise in the difficulties of the parameters' estimation.

1. Introduction

The distribution and transmission lines and their electrical equipment are exposed to many stresses, caused by atmospheric discharges and switching overvoltages, resulting interruption of the normal operation of the electrical network and damage of the equipment. The most common method, in order to improve the lightning performance and reduce the number of faults in high voltage transmission lines, is the installation of overhead ground wires, which intercept lightning strokes, that otherwise will terminate on the phase conductors. Ground wires offer effective protection, when low values of ground resistance are achieved. When lightning strikes the tower structure or overhead shield wire, the lightning discharge current, flowing through the tower and tower footing resistance, produces potential differences across the line insulation. If the line insulation strength is exceeded, flashover occurs, i.e. a backflashover. Since the tower voltage is highly dependent on the tower resistance, consequently footing resistance is an extremely important factor in determining lightning performance [1,2].

Apart from the ground wires, the installation of surge arresters is considered the most effective protection against these transient overvoltages, especially for areas with high ground resistances and keraunic level. The arresters are installed between phase and earth and act as bypath for the overvoltage impulse. They are designed to be insulators for nominal operating voltage, conducting at most few milliamperes of current and good conductors, when the voltage of the line exceeds

* Corresponding author. Tel.: +30 6972702218.
E-mail address: leekonom@gmail.com (L. Ekonomou).

1569-190X/$ - see front matter © 2010 Elsevier B.V. All rights reserved.
doi:10.1016/j.simpat.2010.01.019

design specifications to pass the energy of the lightning strike to the ground. Several different types of arresters are available (e.g. gapped silicon carbide, gapped or non-gapped metal oxide) and all perform in a similar manner: they function as high impedances at normal operating voltages and become low impedances during surge conditions. The conventional silicon carbide arresters with gaps have been replaced in the last years by gapless metal oxide arresters, providing significant advantages, namely:

- superior protective characteristics,
- higher reliability,
- better performance under polluted environment,
- ability to withstand higher temporary overvoltages and
- multiple voltages surges for longer periods of time.

In comparison to arresters with gaps, metal oxide arresters reliably limit the voltage to low values, due to the high non-linearity of the *V–I* characteristic, even for steep impulses, with very fast response time [3–5]. The main characteristics of a surge arrester are [5]: maximum continuous operating voltage (MCOV), which must be greater than the maximum network operating voltage with a safety margin of 5%, rated voltage, which must be 1.25 × MCOV, protection level and capacity to withstand the energy of transient overvoltages.

The adequate circuit representation of metal oxide surge arresters plays an important role in the insulation coordination studies of power systems. The estimation of the arresters failure probability contributes to a more optimum design of a new line or the improvement of an already existing one, intending to a more effective lightning protection, reducing the operational costs and providing continuity of service. Surge arresters improve the lightning performance of the line, but there is also the possibility of damage of the arresters, due to high currents impulses that pass through them. The reduction of the lightning failures of the line after arresters' installation and the failure rate of the arresters, when they absorb energy higher than their absorption capability, are dependent on tower footing resistance, arresters' electrical characteristics, arresters' installation interval, the lightning current waveform and the keraunic level of area [6–11]. The theoretical computation of surge arresters failure probability is also dependent on the selected model for the simulation process. The circuit representation of metal oxide surge arresters is a significant issue, since metal oxide surge arresters present dynamic behavior, mainly dependent on the time to crest of the injected impulse current, i.e. residual voltage reaches its peak before the peak of the impulse current and becomes higher for lower front times of the injected impulse [12].

In this study a review of the most important metal oxide surge arresters is performed. According to the literature various models have been proposed, in order to reproduce the frequency-dependent behavior of metal oxide surge arresters. The most widely used and popular ones are the IEEE model [12], the Pinceti–Gianettoni model [13] and the Fernandez–Diaz model [14]. The last two models are simpler versions of the IEEE model. The arresters models are simulated and compared using an appropriate computer program (PSCAD) presenting and analyzing the effect of each model in the arresters' failure probability calculation.

2. Metal oxide arresters circuit models

Metal oxide arresters present a highly non-linear voltage–current characteristic (Fig. 1), according to the equation [15,16]:

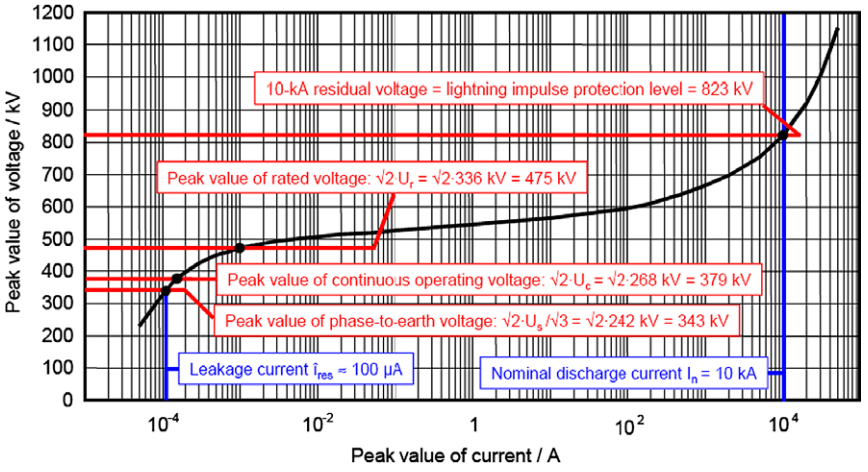

Fig. 1. Metal oxide surge arrester's voltage–current characteristic [4].

$$I = kV^{\alpha}, \quad a > 1 \tag{1}$$

where

I is the current through the arrester,
V is the voltage across the arrester,
a is a non-linearity exponent (measure of non-linearity) and
k is a constant depended on the arresters type.

The value α characterizes the non-linear V–I characteristic; the greater the value of a, the "better" the varistor. Modern arresters have values of α between 25 and 60.

V–I characteristic must be determined using measurements performed with brief pulse currents, such as an 8/20 μs waveshape, in order to avoid effects such as varistor heating. Furthermore, the interval between the consecutive surges in the laboratory must be sufficiently long to allow varistor revert room temperature prior to the application of the consequent surge [17]. Data and measurements on characteristics of metal oxide surge arresters indicate a dynamic behavior. The residual voltage of the arrester depends on the current surge waveform shape and increases as the current front time decreases [12,16,17]. This increase of the residual voltage could reach approximately 6% when the front time of the discharge current is reduced from 8 μs to 1.3 μs [12,18,19].

Based on the above, it can be concluded that metal oxide surge arresters cannot be modeled by only a non-linear resistance, since their response depends on the magnitude and the rate of rise of the surge pulse. Metal oxide arresters behave differently for various surge waveforms, depending each time on the peak and the slope of the overvoltage. Several frequent dependent models have been proposed, in a way that the model simulation results correspond to the actual behavior of the arrester. The existing models [2,6–10] differ in the parameters' estimation procedure, but all are efficient enough to simulate the frequency-depended behavior of the arresters.

2.1. The physical model

The basic varistor model is a general non-frequency-dependent model for metal oxide protective devices, presented in Fig. 2. L is the inductance of conducting leads and C is the capacitance of the device package and zinc oxide material. According to the conduction mechanism of the varistor microstructure, the resistive component of the voltage–current characteristic can be divided into three regions: low, medium and the high-current region. At low currents, the varistor can be treated as a high value resistance R_L, and at very high currents the low value bulk resistance R_B of the zinc oxide grains dominates the varistor response [13,16,20,21].

2.2. The IEEE model

The IEEE Working Group 3.4.11 [12] proposed the model of Fig. 3, including the non-linear resistances A_0 and A_1, separated by a R–L filter. For slow front surges the filter impedance is low and the non-linear resistances are in parallel. For fast front surges filter impedance becomes high, and the current flows through the non-linear resistance A_0.

The inductance L_1 and the resistance R_1 comprise the filter between the two varistors, since the inductance L_0 is associated with magnetic fields in the vicinity of the arrester. R_0 stabilizes the numerical integration and C represents the terminal-to-terminal capacitance. The equations for the above parameters and the per-unit V–I characteristic of the varistors are given in [12]:

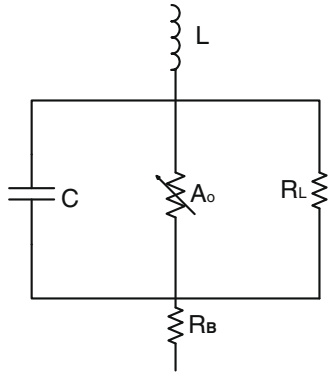

Fig. 2. The physical model.

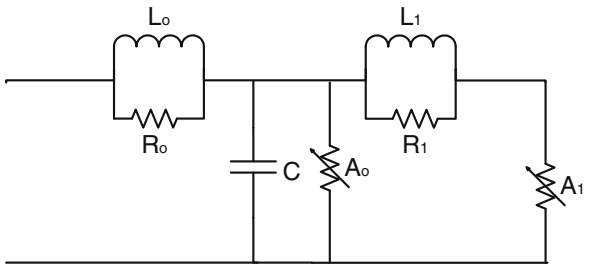

Fig. 3. The IEEE model [12].

$$L_1 = (15d)/n\ \mu\text{H} \tag{2}$$
$$R_1 = (65d)/n\ \Omega \tag{3}$$
$$L_0 = (0.2d)/n\ \mu\text{H} \tag{4}$$
$$R_0 = (100d)/n\ \Omega \tag{5}$$
$$C = (100n)/d\ \text{pF} \tag{6}$$

where

d is the length of arrester column in meters and
n is the number of parallel columns of metal oxide disks.

2.3. The Pinceti–Gianettoni model

This model is based on the IEEE model with some differences. There is no capacitance and the resistances R_0 and R_1 are replaced by one resistance (approximately 1 MΩ) at the input terminals, as shown in Fig. 4. The non-linear resistors are based on the curves of [12]. The inductances L_0 and L_1 are calculated using the equations [13]:

$$L_0 = \frac{1}{4}\cdot\frac{V_{r(1/T_2)} - V_{r(8/20)}}{V_{r(8/20)}}\cdot V_n\ \mu\text{H} \tag{7}$$
$$L_1 = \frac{1}{12}\cdot\frac{V_{r(1/T_2)} - V_{r(8/20)}}{V_{r(8/20)}}\cdot V_n\ \mu\text{H} \tag{8}$$

where

V_n is the arrester's rated voltage,
$Vr_{8/20)}$ is the residual voltage for a 8/20 10 kA lightning current and
$Vr_{1/T2)}$ is the residual voltage for a $1/T_2$ 10 kA lightning current.

The advantage of this model in comparison to the IEEE model is that there is no need for knowing the arresters' physical characteristics, but there is only a need for the knowledge of the electrical data, given by the manufacturer.

2.4. The Fernandez–Diaz model

Based also on IEEE model, A_0 and A_1 are separated by L_1, while L_0 is neglected (Fig. 5). C is added in arrester terminals and represents terminal-to-terminal capacitance of the arrester.

This model does not require iterative calculations since the required data are obtained from the manufacturer's datasheet. The procedure for the computation of the parameters is given in [10]. The V–I characteristics for A_0 and A_1 are calculated using manufacturers' data, considering the ratio I_0 to I_1 equal to 0.02. The inductance L_1 is given as:

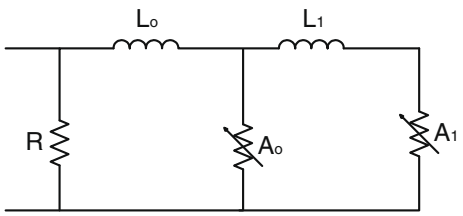

Fig. 4. The Pianceti–Gianettoni model [13].

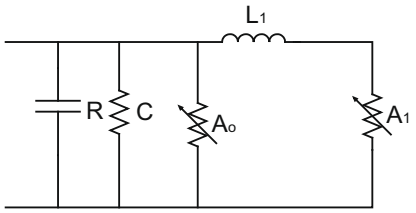

Fig. 5. The Fernandez–Diaz model [14].

$$L_1 = nL_1' \tag{9}$$

where

n is a scale factor and
L_1' is given in [14], computing the percentage increase of the residual voltage as:

$$\Delta V_{res}\ (\%) = \frac{V_{r(1/T_2)} - V_{r(8/20)}}{V_{r(8/20)}} \cdot 100 \tag{10}$$

where

$V_{r(8/20)}$ is the residual voltage for a 8/20 lightning current and,
$V_{r(1/T2)}$ is the residual voltage for a $1/T_2$ lightning current with the nominal amplitude.

3. Simulation results

The simulations for each one model were performed using PSCAD program for a one-column 150 kV MO arrester, with height 952 mm. In Table 1 the electrical and insulation characteristic data of the used surge arrester are given. This type of surge arrester is mainly used in the Hellenic transmission system.

Table 1
Electrical and insulation data of the used in the simulations surge arrester.

MCOV		96 kV
Rated voltage		120 kV
Maximum residual voltage with lightning current 8/20 μs	5 kA	289 kV
	10 kA	312 kV
	20 kA	354 kV
Height		3930 mm
Insulation material		Silicon rubber
Creepage		1428 mm
Energy withstand		1440 kJ

Table 2
Parameters for the physical model.

L	1.52 μH
R_L	1 MΩ
R_B	0.04 Ω
C	107 pF

Table 3
Parameters for the IEEE model.

L_1	14.28 μH
R_1	64.88 Ω
L_0	0.19 μH
R_0	95.2 Ω
C	105.4 pF

Table 4
Parameters for the Pinceti–Gianettoni model.

L_1	2.076 μH
L_0	0.69 μH
R	1 MΩ

Table 5
Parameters for the Fernandez–Diaz model.

L_1	1.07 μH
C	105.4 pF
R	1 MΩ

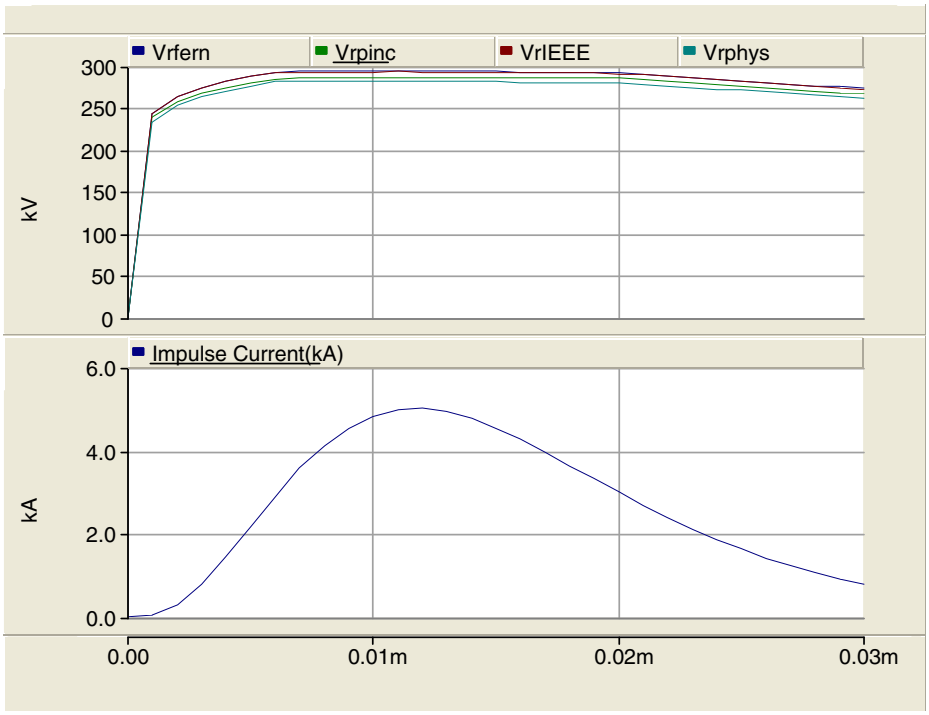

Fig. 6. Residual voltage for a 5 kA current impulse (8/20 μs).

In Tables 2–5 the computed parameters for each one model are shown, according to the procedures described in Section 2.

The residual voltage waveforms of each model for three impulse currents 8/20 μs (5 kA, 10 kA, 20 kA) are shown in Figs. 6–8.

The simulation results for each model are compared with the manufacturer's data (Table 6). The relative error is computed using the equation:

$$e = \frac{Vr_{simulation} - Vr_{manufacturer}}{Vr_{manufacturer}} \cdot 100\% \tag{11}$$

where

$Vr_{simulation}$ is the residual voltage from the simulation and
$Vr_{manufacturer}$ is the residual voltage given by the manufacturer datasheet.

Fig. 9 compares the relative errors (in relation to manufacturer's recorded residual voltage) of the four models at every discharge current level. The physical model and the Pinceti–Gianettoni model seem to underestimate the residual voltage

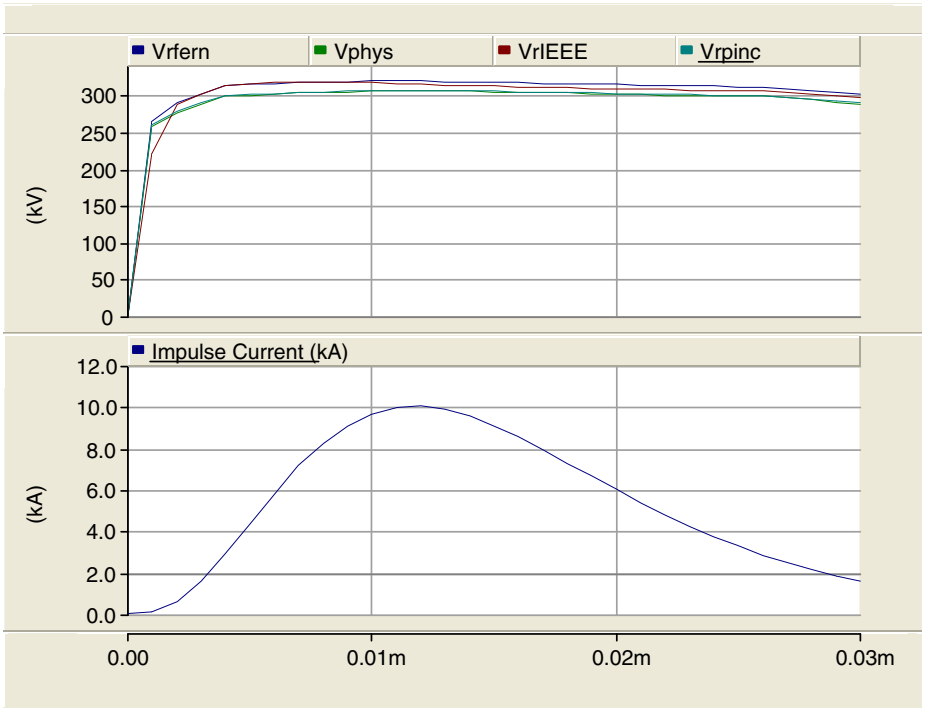

Fig. 7. Residual voltage for a 10 kA current impulse (8/20 μs).

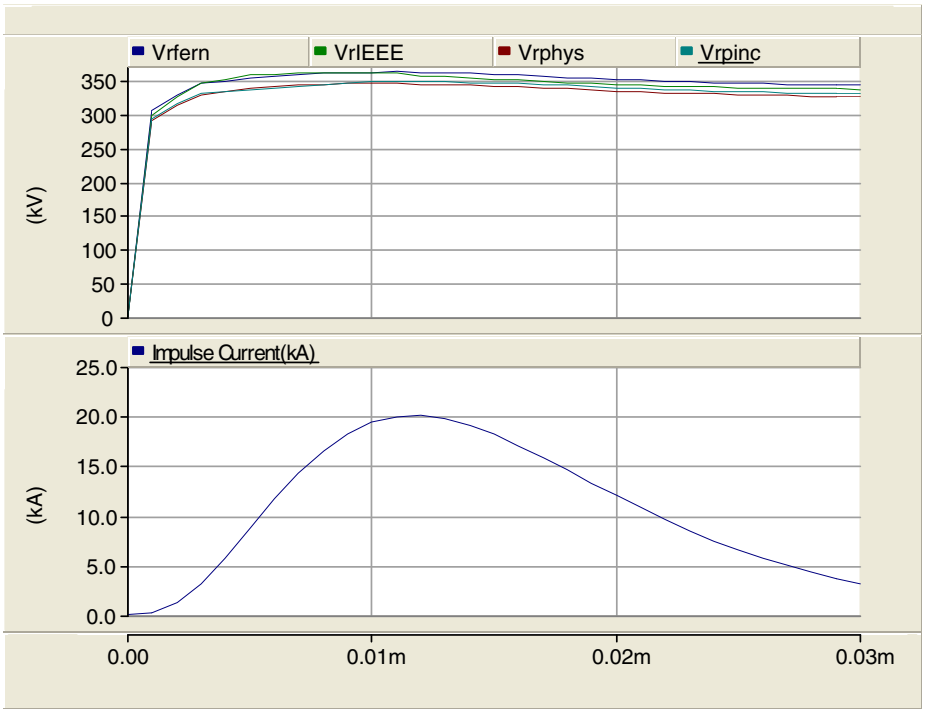

Fig. 8. Residual voltage for a 20 kA current impulse (8/20 μs).

(negative error), in contrast to the other two dynamic models that predict higher residual voltage. It can be observed that the IEEE model presents the lower error, offering higher accuracy, mainly due to its complexity in comparison to the other models.

Table 6
Residual voltages and relative errors for each model.

I (kA)	Residual voltage (kV)								
	Manufacturers' datasheet	Physical model	e (%)	IEEE model	e (%)	Pinceti–Gianettoni model	e (%)	Fernandez–Diaz model	e (%)
5	289	281.94	−2.44	292.96	1.37	282.61	−2.21	293.73	1.63
10	312	304.17	−2.51	316.46	1.43	305.51	−2.08	317.36	1.72
20	354	345.22	−2.48	358.92	1.39	346.42	−2.14	359.91	1.67

The obtained simulation waveform must be as close as possible to the recorded measurements. Therefore, besides the peak residual voltage, the absorbed energy by the arrester must be also checked. This constitutes a very important factor in order to compute the arresters' failure probability. The lightning energy absorbed by an arrester is given by the equation:

$$E = \int_{t_o}^{t} V(t) \cdot I(t) dt \tag{12}$$

where

$V(t)$ is the residual voltage of the arrester in kV and
$I(t)$ is the value of the discharge current through the arrester in kA.

It must be mentioned that when the arrester energy absorption exceeds their withstand capability, the arrester is damaged.

Laboratory measurements obtained from [22] are used in order to show the relationship between the arrester's model selection and the energy absorption. In [22] the absorbed energy of a 7.5 kV surge arrester has been measured and it has been compared with ATP results for the IEEE and the Pinceti–Gianettoni model. In the current study the physical, the IEEE, the Pinceti–Gianettoni and the Fernandez–Diaz models are simulated using PSCAD, following the same procedure that has been used for the 150 kV arrester (Figs. 6–8, Table 6). Table 7 shows the recorded [22] and the calculated absorbed by the arrester energy for each of the examined model.

The small difference between the computed results and those presented in [22] are a consequence of the different computer simulation tools used (ATP vs PSCAD). All the simulated models are able to reproduce with good accuracy the residual voltage and the absorbed energy. Although the Fernandez–Diaz model gives in general greater peak residual voltage values, the IEEE model absorbs more energy; this is owned to the shape of the waveform, since the area under the residual voltage curve is bigger for the IEEE model. The advantage of the three dynamic models, apart from the fact that they decrease the relative error, is that they can represent the frequency-dependent behavior of the metal oxide surge arrester, which is really important when the time to crest value of the lightning current is not constant.

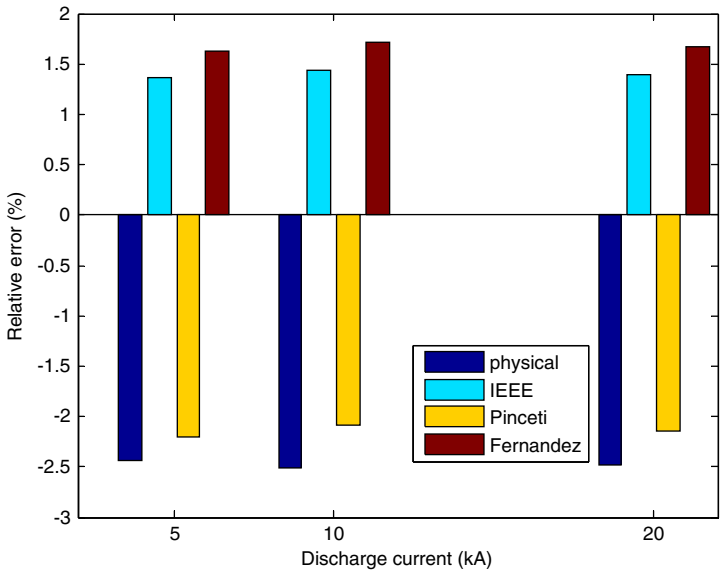

Fig. 9. Relative errors of the residual voltage for each model.

Table 7
Absorbed energy for each examined model.

Measurement	Physical model	e (%)	IEEE model	*e* (%)	Pinceti–Gianettoni Model	*e* (%)	Fernandez–Diaz model	*e* (%)
6413.1 J	6269.4 J	−2.24	6501.7 J	1.38	6487.3 J	1.15	6499.2 J	1.34

4. Evaluation of arresters failure probability using the equivalent circuit models

The use of the proposed arrester circuit models for lightning performance studies offers more reliable and accurate results, in comparison to the simple non-linear resistance model that the various program tools include in their libraries, since these dynamic frequency-dependent models represent more efficiently the residual voltage waveform. The four models, presented in Section 2, are implemented, using an appropriate computer program, in Hellenic high voltage transmission lines. Arresters' failure probability is computing with the use of each model, taking into consideration parameters such as the installation interval and the tower footing resistance. In more detail, the arrester's failure probability depends on:

a. their energy absorption capability, which is the maximum level of energy injected into the arrester, at which it can still cool back down to its normal operating temperature.

b. the installation interval, the distance in which surge arresters are installed. In regions with high keraunic level and grounding resistance a more dense arresters installation is required.

c. the tower footing resistance, for direct strikes to phase conductors, low tower footing resistance results in higher energy through the arrester; for strikes on towers or on ground wires, high resistances increase the arresters failure probability.

d. the electrogeometrical model: when the downward leader approaches to earth, the point that the leader will hit depends on the magnitude of the lightning stroke current. The electrogeometrical model represents this idea by using the striking distance concept, for the ground wire or the ground. Considering $r_{c,g} = aI^b$, is designed the model of Fig. 10 [23].

The probabilities $h_A(I_P)$ and $h_B(I_P)$ that the lightning strikes a phase conductor or the overhead ground correspondingly, can be estimated for each value of the peak current I_P using Eqs. (13) and (14):

$$h_A(I_p) = \frac{X_C}{X} \tag{13}$$

$$h_B(I_p) = \frac{X - X_C}{X} \tag{14}$$

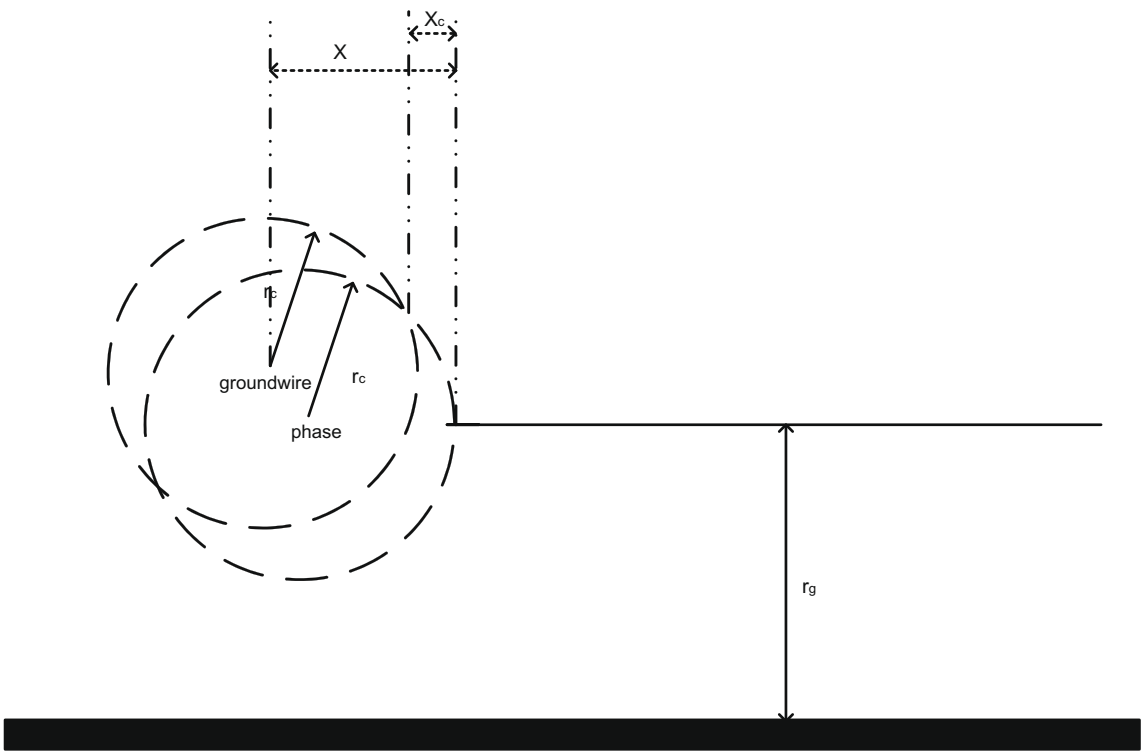

Fig. 10. Electrogeometrical model: representation of ground wires and phase conductors [23].

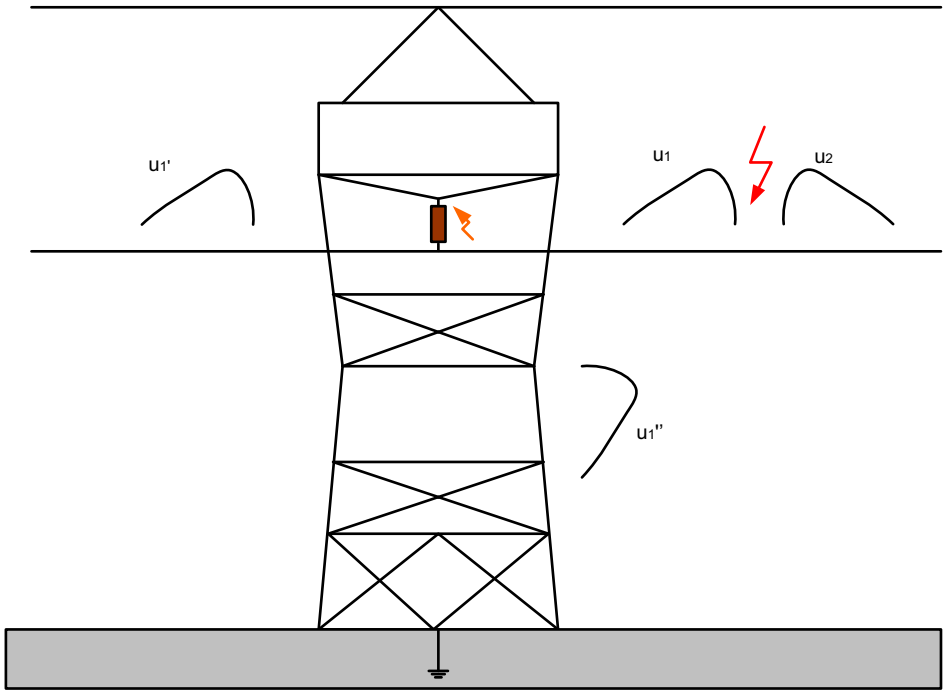

Fig. 11. Shielding failure on a transmission line.

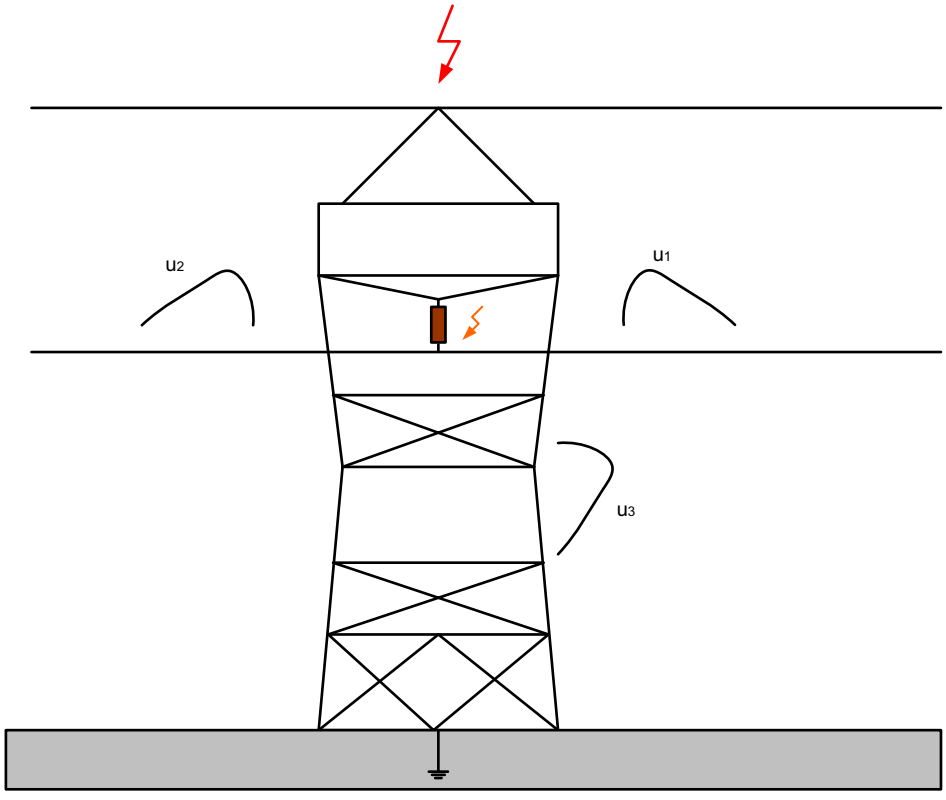

Fig. 12. Backflashover failure on a transmission line.

All the above factors are summarized in the following equation [6–11]:

$$P = \int_{T_r}^{\infty} \left\{ \int_{I_A(T_t)}^{\infty} f(I_p) \cdot h_A(I_P) dI_P \right\} g(T_t) dT_t + \int_{T_t}^{\infty} \left\{ \int_{I_B(T_t)}^{\infty} f(I_P) \cdot h_B(I_P) dI_P \right\} g(T_t) dT_t \tag{15}$$

where: P is the total failure probability of an arrester, $I_A(T_t)$ is the minimum stroke peak current in kA required to damage the arrester, when lightning hits on a phase conductor, depending on each time-to-half value, $I_B(T_t)$ is the minimum stroke peak current in kA required to damage the arrester, when lightning hits on the overhead ground wire, depending on each time-to-half value, $f(I_P)$ is the probability density function of the lightning current peak value, $g(T_t)$ is the probability density function of the time-to-half value of the lightning current and T_r is the rise time of the incident waveform,

Figs. 11 and 12 show lightning strokes on the phase conductor or on ground wire, correspondingly, for a high voltage transmission line. When lightning hits the tower or the ground wire, an increase on the potential of the metal structure of the tower is caused (depending on the grounding resistance) up to the critical flashover voltage that leads to a backflashover. The possibility of a shielding failure, i.e. a failure due to a lightning hit on the phase conductor, is small, since lightning currents that strike the protected conductors are not high enough, according to the electrogeometrical model.

Surge arresters are installed between the phase conductors and earth, in order to prevent the flashovers along the insulators. In case of direct stroke on phase conductors, the surge arrester becomes conductive, leading the overvoltage current to the ground. When lightning strikes the tower or the ground wires (Fig. 13), one part travels in both directions of the ground wire (u_1 and u_2), one part goes down to the grounding system (u_3), and one part flows through the arrester, which conducts backwards, to the line, splitting also to both directions (u_4 and u_5). The sharing of the lightning current depends mainly on the tower footing resistance. The voltage wave travelling along the phase conductor may cause flashover to the next tower hence the installation of surge arresters with a dense step is necessary, especially in regions with high keraunic level and high grounding impedances, in order to divert the remaining overvoltage wave to the ground (u_6). This will continuously occur from one tower to another (u_7), until all the lightning current is diverted to earth.

The waveform of the lightning surge has been produced by a double exponential wave, considering the time to crest value constant at 2 μs. The peak current and time-to-half distribution functions used, are those performed by Berger in Monte San Salvatore [11]. The surge impedance values are 400 Ω for phases and 700 Ω for ground wires. The towers are represented as distributed parameters lines 200 Ω. In the simulation, surge arresters are installed on all phases and three cases are tested. In

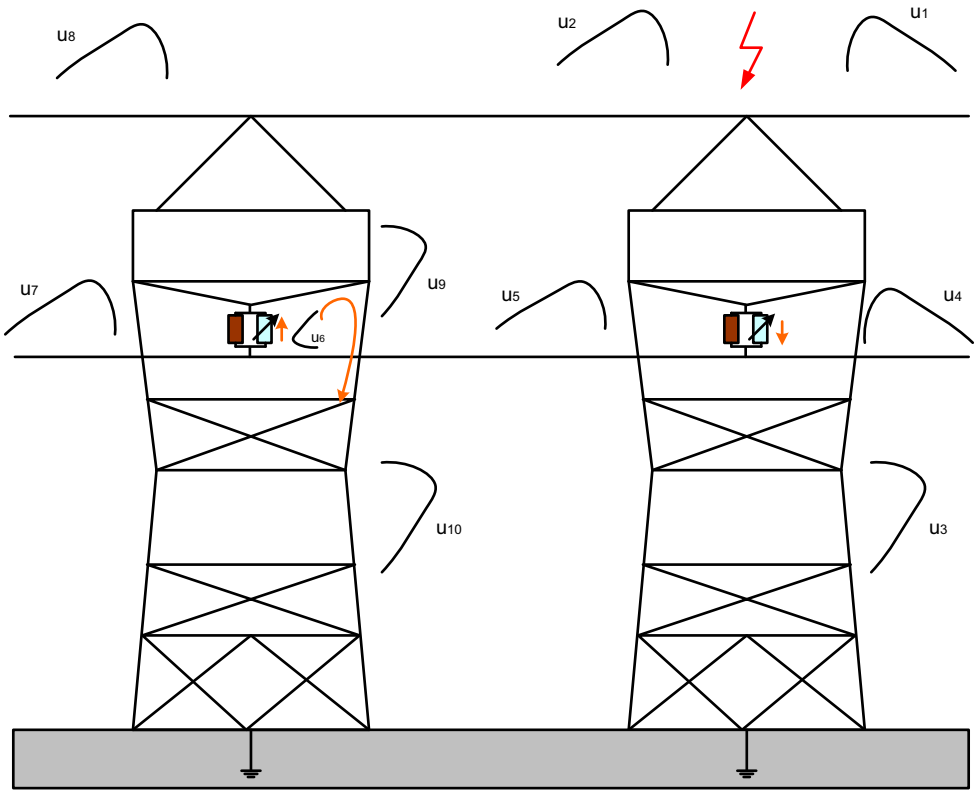

Fig. 13. Arresters conduction for a lightning stroke on the tower.

Table 8
Arresters failure probability for each one case and each one model.

TFR	P_1 (%)	P_2 (%)	P_3 (%)	P_1 (%)	P_2 (%)	P_3 (%)
	Physical model			*IEEE*		
20 Ω	0.144	0.306	0.464	0.183	0.378	0.588
40 Ω	0.216	0.374	0.539	0.267	0.447	0.627
60 Ω	0.287	0.425	0.584	0.357	0.521	0.663
80 Ω	0.403	0.536	0.705	0.478	0.629	0.841
120 Ω	0.714	0.751	0.827	0.851	0.902	0.935
	Pincetti–Gianettoni			*Fernandez–Diaz*		
20 Ω	0.167	0.344	0.522	0.178	0.352	0.579
40 Ω	0.238	0.402	0.589	0.252	0.425	0.612
60 Ω	0.330	0.478	0.625	0.349	0.492	0.642
80 Ω	0.439	0.596	0.792	0.465	0.607	0.814
120 Ω	0.776	0.843	0.900	0.792	0.895	0.916

Case 1 arresters are installed on every tower, in Case 2 arresters are installed on every second tower and in Case 3 arresters are installed on every third tower.

The waveforms of the arresters' terminal voltage and the current flowing through them are used in order to calculate the energy dissipated by the arresters. The arresters failure probability is computed using (15). In order to find the minimum stroke currents for each time-to-half value $I_A(T_t)$ and $I_B(T_t)$, required for the arresters' failure, an arithmetic method programmed in Matlab is used, properly combined with PSCAD simulation procedures. Considering a stroke on phase or on ground wires, for each time-to-half value the lighting current that damages the arresters is calculated, with a time-to-half range from 10 μs to 1000 μs and step 1 μs.

In Table 8 the results for various tower footing resistance values are given. The failure probability increases as grounding resistance increases, in the same way for all the models. An arrester's failure can be caused by a lightning strike to a phase conductor, to the tower or to the overhead ground wire. For direct strikes to phase conductors, low tower footing resistance results in higher energy through the arrester; for strikes on towers or on ground wires, high resistances increase the arresters failure probability. The probability of failure due to strike on phases is small, so strike on ground wire is the dominant case for the determination of the arresters' failure rate.

Fig. 14 shows the arresters failure probability in relation to the tower footing resistance, for the IEEE model, for the three analyzed case studies. It can be observed that smaller arrester installation interval decreases the arresters failure rate. Therefore for regions with high tower footing resistance, arresters installation on every tower is recommended.

Fig. 15 presents the arrester failure probability in relation to the tower footing resistance for all models, when the arresters are installed on every tower (Case 1). Although the Fernandez–Diaz model gives greater peak value of the residual voltage, the IEEE model gives a little greater probability, mainly due to the fact that the area under the voltage curve is bigger, so

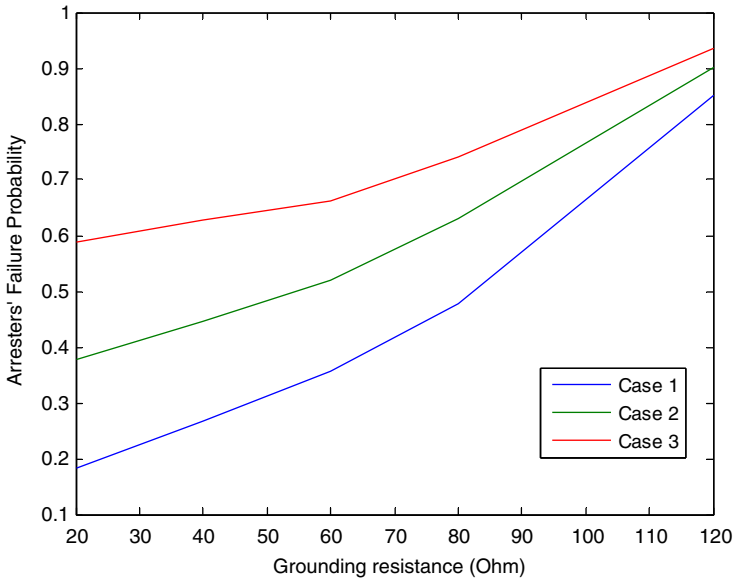

Fig. 14. Arrester's failure probability versus tower footing resistance for the IEEE model and for each one of the three analyzed case studies.

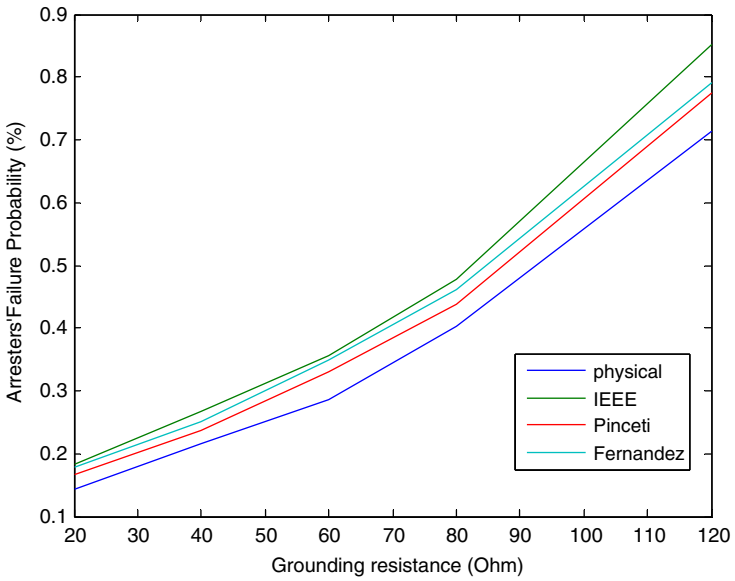

Fig. 15. Arresters failure probability versus tower footing resistance for all models and for arresters installed on every tower.

the absorbed energy will be greater. As expected, the physical model gives the lowest failure probability, since computes lower residual voltage (Table 6) and absorbed energy (Table 7). The comparison with field inspection data for the annual failure rate of the arresters installed on a line will be useful for the study of the models' accuracy. However, the computed results show that all models are appropriate for lightning performance simulation and failure probability estimation. Thus the selection of the most suitable model for a study depends on the available data.

5. Conclusions

This study presents a review of the most used frequency-depended models for metal oxide surge arresters. The residual voltage and the absorbed energy for each model applying impulse currents were computed using PSCAD, and the simulation predictions were compared with real measured data. All models represent successfully the arresters' lightning behavior, presenting an acceptable error. However, the physical model is the only one that cannot represent the dependence of the residual voltage peak with the time to crest value. Therefore the use of the dynamic models, which reproduce more efficiently the real behavior of the metal oxide surge arresters, is suggested. Furthermore the computation of the energy injected to the arrester is a very important issue, since it is an indicator of the curve-fitting of the simulated and the measured waveform and affects the estimation of the arrester's failure probability. Finally, the models were also used in order to estimate the arrester's failure probability of a 150 kV Hellenic transmission line. The analysis showed that the three frequency-dependent models have an efficient dynamic behavior and can be used to estimate the lightning performance of high voltage transmission lines. Finally it has been proved that the decision on which model should be used depends on the available data, the complexity of the system and the demanded speed of the simulation, since the Pinceti–Gianetoni and the Fernandez–Diaz model are simpler than the IEEE model.

References

[1] IEEE Working Group on Lightning Performance of Transmission Lines, A simplified method for estimating lightning performance of transmission lines, IEEE Trans. Power Appl. Syst. PAS-104(April) (1985) 919–932.
[2] J.A. Martinez, F. Castro-Aranda, Lightning performance analysis of overhead transmission lines using the EMTP, IEEE Trans. PWRD 20 (3) (2005) 294–300.
[3] ABB Buyer's Guide, High Voltage Surge Arresters, Edition 5.1, 2004–2007.
[4] V. Hinrichsen, Metal-Oxide Surge Arresters, Siemens, first ed., 2001.
[5] IEC 60099-4, Surge Arresters: Part 4: Metal-Oxide Surge Arresters Without Gaps for a.c. Systems, second ed., 2004–2005.
[6] J.A. Tarchini, W. Gimenez, Line surge arrester selection to improve lightning performance of transmission lines, IEEE Bologna PowerTech Conference, Bologna, Italy, 2003.
[7] L. Montanes, M. Garcia-Gracia, M. Sanz, M.A. Garcia, An improvement for the selection of surge arresters based on the evaluation of the failure probability, IEEE Trans. Power Delivery 17 (1) (2002) 123–128.
[8] M. Garcia-Gracia, S. Baldovinos, M. Sanz, L. Montanes, Evaluation of the failure probability for gapless metal oxide arresters, in: IEEE Transmission and Distribution Conference, 1999.
[9] K. Nakada, S. Yokoyama, T. Yokota, A. Asakawa, T. Kawabata, Analytical study on prevention for distribution arrester outages caused by winter lightning, IEEE Trans. Power Delivery 13 (4) (1998) 1399–1404.

[10] L.C. Zanetta, C.E. de M. Pereira, Application studies of line arresters in partial shielded 138-kV transmission lines, IEEE Trans. Power Delivery 18 (1) (2003) 95–100.
[11] K. Berger, R.B. Anderson, H. Kroninger, Parameters of lightning flashes, Electra 41 (1975) 23–37.
[12] IEEE Working Group 3.4.11, Modeling of metal oxide surge arresters, IEEE Trans. Power Delivery 7(1) (1992) 302–309.
[13] P. Pinceti, M. Giannettoni, A simplified model for zinc oxide surge arresters, IEEE Trans. Power Delivery 14 (2) (1999) 393–398.
[14] F. Fernandez, R. Diaz, Metal oxide surge arrester model for fast transient simulations, in: International Conference on Power System Transients (IPAT'01), Rio De Janeiro, Brazil, 2001, Paper 14.
[15] R.B. Standler, Protection of Electronic Circuit from Overvoltages, John Wiley & Sons, 1989.
[16] B. Žitnik, M. Žitnik, M. Babuder, The ability of different simulation models to describe the behavior of metal oxide varistors, in: 28th International Conference on Lightning Protection, Kazanaqa, Japan, 2006, pp. 1111–1116.
[17] A. Bayadi, N. Harid, K. Zehar, S. Belkhiat, Simulation of metal oxide surge arrester dynamic behavior under fast transients, in: International Conference on Power Systems Transients, New Orleans, USA, 2003.
[18] G.L. Goedde, L.A. Kojovic, J.J. Woodworth, Surge arrester characteristics that provide reliable overvoltage protection in distribution and low voltage systems, in: IEEE Power Eng. Society Summer Meeting, vol. 4, 2000, pp. 2375–2380.
[19] I. Kim, T. Funabashi, H. Sasaki, T. Hagiwara, M. Kobayashi, Study of ZnO surge arrester model for steep front wave, IEEE Trans. Power Delivery 11 (2) (1996) 834–841.
[20] N. Suljanovic, A. Mujcic, V. Murko, Practical issues of metal-oxide varistor modeling for numerical simulations, in: 28th International Conference on Lightning Protection, Kazanaqa, Japan, 2006, pp. 1149–1154.
[21] A. Bayadi, N. Harid, K. Zehar, S. Belkhiat, Simulation of metal oxide surge arrester dynamic behavior under fast transients, in: International Conference on Power Systems Transients, New Orleans, USA, 2003.
[22] G.R.S. Lira, D. Fernandes Jr., E.G. Costa, Computation of energy absorption and residual voltage in metal oxide surge arrester from digital models and lab tests: a comparative study', in: International Conference on Power Systems Transients (IPST'07), Lyon, France, 2007.
[23] IEEE Working Group on Lightning Performance on Transmission Lines, A simplified method for estimating lightning performance of transmission lines, IEEE Trans. PAS 104(4) (1985) 917–927.